An Affinity-Based Workflow for Clusterin Purification and Interactome Characterisation in Human Plasma

AUTHOR NAMES

Amalia Kontochristou, Nika Šimičić, Anouk M. Rijs, and Melissa Baerenfaenger*

AUTHOR ADDRESS

Amalia Kontochristou − Division of Bioanalytical Chemistry, Department of Chemistry and Pharmaceutical Sciences, Amsterdam Institute of Molecular and Life Sciences, Vrije Universiteit Amsterdam, 1081 HV Amsterdam, The Netherlands; Centre for Analytical Sciences Amsterdam (CASA), The Netherlands; orcid.org/0009-0006-5988-0024

Nika Šimičić − Division of Bioanalytical Chemistry, Department of Chemistry and Pharmaceutical Sciences, Amsterdam Institute of Molecular and Life Sciences, Vrije Universiteit Amsterdam, 1081 HV Amsterdam, The Netherlands; Centre for Analytical Sciences Amsterdam (CASA), The Netherlands; Center for Proteomics and Metabolomics, Leiden University Medical Center, Leiden 2333, ZA, The Netherlands; orcid.org/0009-0000-4381-6219

Anouk M. Rijs − Division of Bioanalytical Chemistry, Department of Chemistry and Pharmaceutical Sciences, Amsterdam Institute of Molecular and Life Sciences, Vrije Universiteit Amsterdam, 1081 HV Amsterdam, The Netherlands; Centre for Analytical Sciences Amsterdam (CASA), The Netherlands; orcid.org/0000-0002-7446-9907

Melissa Baerenfaenger − Division of Bioanalytical Chemistry, Department of Chemistry and Pharmaceutical Sciences, Amsterdam Institute of Molecular and Life Sciences, Vrije Universiteit Amsterdam, 1081 HV Amsterdam, The Netherlands; Centre for Analytical Sciences Amsterdam (CASA), The Netherlands; orcid.org/0000-0002-2855-924

KEYWORDS

Affinity purification, Chaperone, Clusterin, Human plasma, Protein interactome

ABSTRACT Clusterin is an extracellular chaperone protein involved in maintaining proteostasis by binding to unfolded or misfolded proteins to prevent their aggregation. Its chaperone activity plays a significant role in human health, as seen in Alzheimer's disease, where clusterin co-localises with amyloid-β plaques to facilitate their clearance. However, its strong tendency to "cluster" with a wide range of client proteins and its low abundance in biological matrices, complicate its purification and characterisation, often resulting in co-isolation of interacting proteins. To enable comprehensive analysis of clusterin, we established two affinity-based purification workflows, one clusterin enrichment and a second for interactome characterisation in human plasma, using a commercial clusterin resin combined with bottom-up proteomics. Systematic optimisation of the purification workflow revealed that increasing ionic strength and adding a non-ionic detergent reduced non-specific protein-protein interactions, thereby improving clusterin enrichment while minimising co-purification. In contrast, omitting these disruptive conditions preserved native protein-protein interactions, enabling the development of the second workflow for clusterin interactome analysis by affinity purification-mass spectrometry. Bottom-up proteomics profiling revealed clusterin-associated proteins involved in immune response, hemostasis, and high-density lipoprotein (HDL)-

associated pathways. Together, these complementary workflows enables targeted clusterin purification and interactome analysis, offering new insights into clusterin's biological roles in human plasma.

Introduction

Clusterin (CLUS) is a glycosylated protein with a molecular weight of 60-85 kDa, expressed both intracellularly and extracellularly across almost all tissues and biofluids[1], including plasma, cerebrospinal fluid, saliva, and urine[2]. As a molecular chaperone, clusterin binds to hydrophobic regions exposed on misfolded or stress-damaged proteins, such as amyloid-β, α-synuclein, and Tau[3–6], and either stabilises them or promotes their degradation[7,8]. By shielding these hydrophobic segments, clusterin suppresses protein aggregation and limits the pathological accumulation of amyloidogenic proteins in cells and biofluids, making it an attractive target for studying mechanisms of neurodegeneration in Alzheimer's disease and Parkinson's disease[9,10]. Beyond its chaperone role, clusterin participates in various other biological processes, including modulation of inflammation via negative regulation of the complement system[11], association with fibrin clots during blood coagulation[12], transport of proteins across the blood-brain barrier[13], and incorporation into high-density lipoprotein particles in plasma[2,14]. Due to its broad tissue distribution, diverse structure, and functional versatility, clusterin has been the focus of many studies[15–18]. Yet its purification from biological samples remains challenging.

Various approaches have been employed to purify clusterin from human plasma, consistently highlighting the challenge posed by both the intrinsic complexity of the biofluid[19] and clusterin's known ability to form complexes with a wide range of proteins[20–22], including immunoglobulins, apolipoproteins, and complement components[23,24], that further complicates its isolation. Human plasma contains thousands of proteins spanning a wide dynamic range,

with a small number of highly abundant species, such as albumin and immunoglobulin G, accounting for more than 90% of the total protein content[19,25]. In contrast, clusterin is present in plasma at substantially lower levels, such that without prior enrichment, detection and characterisation are severely hindered by dominant plasma proteins[26]. To address these challenges, many purification protocols rely on immunoaffinity enrichment[27,28] using monoclonal or polyclonal antibodies, which provide high binding specificity for clusterin[29,30], often in combination with complementary chromatographic techniques, such as size-exclusion chromatography[30], ion-exchange chromatography[31], and hydrophobic interaction chromatography[32]. These techniques preserve the native structure of clusterin and consequently maintain its chaperone activity, which is crucial for functional studies or interactome analysis. However, the retained chaperone activity complicates purification, as clusterin continues to bind its client proteins, resulting in extensive co-purification[33]. This obstacle was also observed by Gordon *et al*., who co-purified clusterin with several plasma proteins despite optimised separation, highlighting the difficulty of isolating clusterin in its native form due to its chaperone function[34].

To overcome these challenges, we established a workflow that integrates immunoaffinity enrichment and bottom-up proteomics to optimise clusterin purification and enable characterisation of its interaction network in human plasma. Clusterin enrichment was achieved using a commercially available clusterin-specific affinity resin containing recombinant single-domain antibody fragments comprising solely the variable-heavy domain, and was implemented in two modes. Under protein-protein interaction-disruptive conditions that minimise ionic and hydrophobic interactions, the workflow enabled selective purification of clusterin. In contrast, when operated under milder, non-disruptive conditions, the same workflow was used for interactome profiling by affinity purification mass spectrometry (AP-MS). AP-MS is a well-established technique for mapping protein-protein interactions, in which

a bait protein, in this case clusterin, is isolated along with its binding partners[35], thereby enabling the detection of stimulus- and condition-dependent protein associations[36,37]. This workflow therefore provides complementary insight into both the selectively enriched protein and its dynamic interaction network in plasma, thereby informing its functional role in health and disease.

Materials and Methods

Purification of human plasma CLUS

Pooled human plasma (S4180-100) was sourced from Biowest SAS (Nuaillé, France). For the enrichment of clusterin from 50 µL of human pooled plasma, 100 µL of POROS™ CaptureSelect™ ClusterinClear Affinity Resin (10 mL), kindly provided by Thermo Fisher Scientific (Carlsbad, CA, USA), was used. The clusterin affinity resin was transferred into a Pierce™ Micro-Spin Column supplied by Thermo Fisher Scientific (Rockford, USA). Before applying the plasma sample, the resin was first washed with Milli-Q water and equilibrated with Dulbecco's Phosphate Buffered Saline (DPBS, pH 7.4) supplied by Thermo Fisher Scientific (Paisley, UK). Milli-Q water was produced by a Millipore purification system (Millipore, Amsterdam, The Netherlands). Human plasma was then diluted 1:1 with DPBS and loaded onto the equilibrated resin. To remove the unbound proteins, the resin was washed multiple times with DPBS buffer and Milli-Q water. Additional wash steps with sodium chloride (NaCl) and Tween 20, supplied by Sigma-Aldrich (St. Louis, USA), were implemented to minimise protein-protein interaction. Following the washing steps, clusterin was eluted from the affinity material with 100 µL of glycine buffer (pH 2.3), and the eluate was neutralised with 40 µL of Tris(hydroxymethyl)aminomethane (Tris) buffer (pH 9.0), both supplied by Sigma-Aldrich (St. Louis, USA). The sample was then dried under vacuum and

stored at −20 °C before bottom-up proteomics analysis. The different purification protocols used are summarised in Table S1.

Bottom-up proteomics

The clusterin-enriched sample was subjected to tryptic digestion. For this, the sample was redissolved in 5 µL of 5 M guanidine hydrochloride and 10 µL of 50 mM DL-dithiothreitol, followed by an incubation at 37 °C with shaking at 650 rpm for 20 minutes. Subsequently, 10 µL of 50 mM iodoacetamide was added, followed by a 60-minute incubation in the dark. Then, 60 µL of 50 mM ammonium bicarbonate and 1 µL of Trypsin/Lys-C (1 mg/mL), supplied by Promega Benelux B.V. (Leiden, The Netherlands), were added, and the sample was incubated overnight at 37 °C with shaking at 650 rpm. Trypsin was inactivated by a five minutes incubation at 90 °C. After tryptic digestion, the sample was stored at -20 °C prior to analysis.

Liquid chromatography tandem mass spectrometry (LC-MS/MS) analysis was performed using an Agilent 1290 Infinity II system (Agilent Technologies Netherlands B.V., Middelburg, The Netherlands) coupled to a trapped ion mobility quadrupole time-of-flight (timsTOF Pro 2) mass spectrometer equipped with an electrospray ionisation (ESI) source operating in positive ion mode (Bruker Daltonics, Bremen, Germany). LC separation was performed at 55 °C with a flow rate of 80 µL/min using solvent A (0.1% formic acid (FA) in water) and solvent B (0.1% FA in acetonitrile). The column used was an Acclaim PepMap 100 C18 reversed-phase column (1 mm ID × 150 mm length, 3 µm particles, 100 Å pore size) supplied by Thermo Fisher Scientific (Ermelo, The Netherlands). The gradient was set as follows: 0 min, 3% B; 2 min, 3% B; 37.5 min, 40% B; 38 min, 90% B; 43.5 min, 90% B; and 60 min, 2% B. Prior to sample injection, mass and mobility calibration were performed using Agilent Technologies ESI-L tuning mix ions. For MS analysis, the DDA PASEF-standard_1.1sec_cycletime.m Bruker

application method was used, with adapted ESI source settings [38]. More information on the MS settings is provided in Table S2.

Data Processing

For data analysis, FragPipe v23.0, MSFragger version 4.3, and Philosopher v5.1.1 were used[39]. Label-free quantification with match between runs (LFQ-MBR) was performed using the IonQuant workflow (version 1.11.11). The UniProt ID UP000005640 database downloaded on 9 December 2023 was used. Precursor mass tolerance was set at ±20 ppm, and trypsin and Lys-C were selected as the enzymes for proteolytic digestion. Carbamidomethylation of cysteine was set as a fixed modification, while methionine oxidation, pyroglutamic acid formation, or loss of ammonia at the peptide N-terminus, and N-terminal acetylation were specified as variable modifications. For MS1 quantification, the MaxLFQ minimum ions was set to 3, the match-between-runs ion false discovery rate (MBR ion FDR) was set to 0.01, and peptide-protein uniqueness was restricted to unique only.

The generated data was processed and visualised using in-house developed Python scripts, which are available upon request. To visualise the distribution of protein abundances across the samples, MaxLFQ intensity values were used. For each protein, the mean MaxLFQ intensities were calculated across replicates, and proteins with non-positive mean values were excluded. Then, the mean intensities were $\log_{10}$-transformed, sorted in descending order, and plotted as abundance rank versus $\log_{10}$(MaxLFQ intensity) using matplotlib.pyplot library version 3.10.0.

For bar plot generation, the relative abundance of clusterin was calculated for each replicate as the percentage of its MaxLFQ intensity relative to the total MaxLFQ intensity across all proteins within the sample. Relative clusterin abundances were summarised across

experimental conditions and visualised as bar plots using seaborn version 0.13.2 and matplotlib.pyplot libraries.

For the volcano plots, MaxLFQ protein intensities were $\log_2$-transformed, and median-centred normalisation was applied per condition to correct for systematic variation. Missing values were imputed per condition using a normal distribution with a downshift of 1.8 standard deviations and a width of 0.3 times the standard deviation of the observed values, following a Perseus-style approach. Welch's t-test was used to compare conditions, and $\log_2$ fold changes (FC) were calculated from the mean normalised intensities. Volcano plots were generated using the seaborn and matplotlib libraries, with $\log_2$ FC on the x-axis and $-\log_{10}$ (p-value) on the y-axis. Proteins with $|\log_2 FC| \geq 1$ and $p < 0.05$ were considered significantly enriched.

To define the interactome of clusterin, proteins significantly enriched in the clusterin purification relative to human plasma, as identified by volcano plot analysis, were selected and analysed using the STRING database version 12.0. Details of the STRING parameters and settings used for network generation are provided in the Supporting Information (Table S3).

Results and Discussion

Clusterin affinity purification

Clusterin was purified from human plasma using a clusterin affinity resin containing immobilised antibodies for capturing clusterin in a solid-phase extraction (SPE) setup. The purification process can be summarised into three main steps, as shown in Figure 1. First, the sample was loaded onto the affinity resin, allowing clusterin to bind to the immobilised antibody. This was followed by a series of washing steps to remove unbound components. Finally, clusterin was eluted from the affinity resin by lowering the pH, thereby disrupting the antibody–antigen binding.

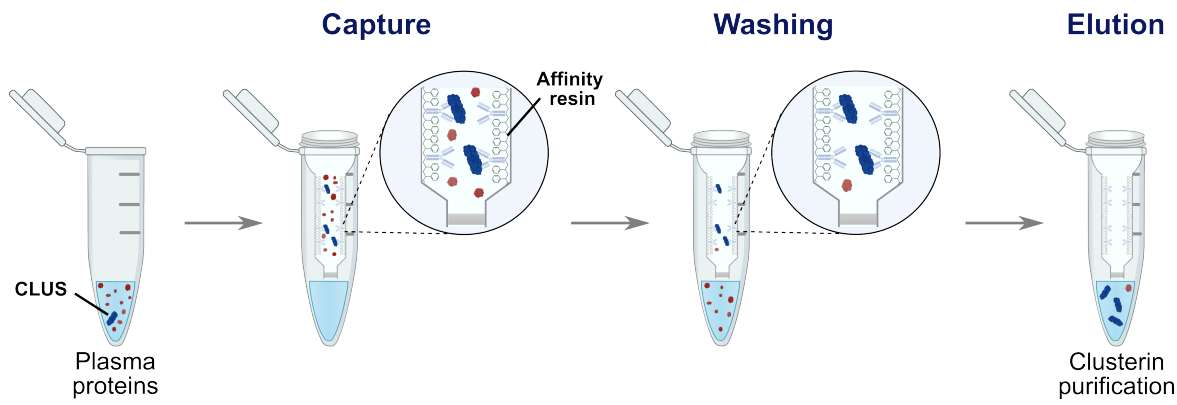

Figure 1: Clusterin purification workflow using POROS™ CaptureSelect™ ClusterinClear affinity resin. The purification was performed in a spin column and involved three sequential steps. Capture: Human plasma was applied to the affinity resin, where clusterin (in blue) bound selectively to the immobilised antibody. Washing: Unbound plasma proteins (in red) were removed during the washing step. Elution: The interaction between clusterin and the antibody was disrupted, resulting in clusterin elution.

The initial clusterin purification protocol evaluated in this study, referred to as Protocol 1, was established according to the supplier's instructions for the clusterin affinity resin and adapted for an SPE approach. Similar conditions have also been applied in previous studies, both for the affinity purification of clusterin complexes[24], and for the purification of other human proteins, such as immunoglobulins[40,41]. According to Protocol 1, DPBS buffer at pH 7.0–7.5 was used as the equilibration buffer to adjust the pH of both the resin and the plasma sample within the recommended range (pH 6–8) prior to sample loading. After sample loading, the resin was washed with DPBS buffer to remove unbound plasma components while retaining clusterin bound to the affinity resin. Finally, clusterin was eluted using a low-pH solution, specifically 0.1 M glycine at pH 2.3, thereby disrupting the clusterin-antibody interaction and releasing the target protein. The purified samples were subsequently subjected to proteolytic digestion and analysed by bottom-up proteomics using label-free quantification (LFQ).

To assess the effectiveness of the purification, the relative abundance of proteins in the purified sample was compared with that in non-enriched human plasma. For this purpose, the $\log_{10}$ MaxLFQ intensities of all identified proteins were plotted against their abundance ranks to illustrate the dynamic range of protein abundances. As shown in Figure 2, Protocol 1 resulted in significant purification of clusterin compared to the non-enriched plasma, as indicated by the decrease in clusterin's abundance rank and by the reduced total number of proteins detected after purification. However, despite the use of a clusterin-specific affinity resin, a significant number of proteins co-purified with clusterin (Figure 2B). Proteins such as albumin (ALBU), immunoglobulin (IGHG1), apolipoprotein (APOA1), and fibrinogen (FIBB) remained more abundant than clusterin even after purification, potentially due to their inherent high abundance in human plasma, suggesting that further purification was required.

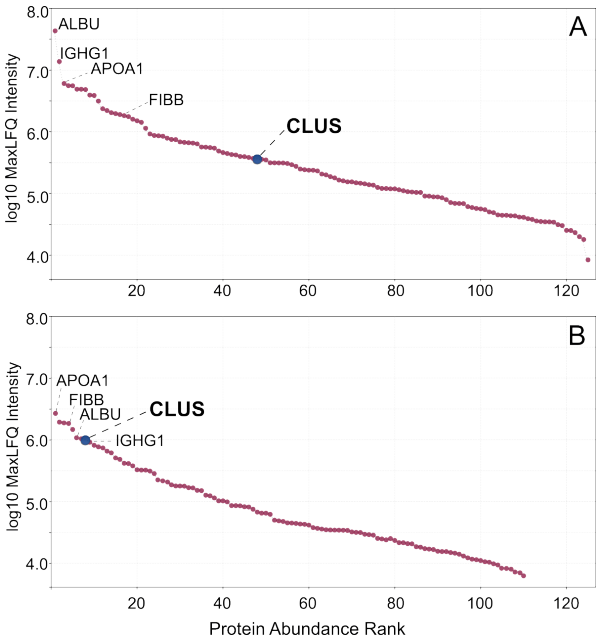

Figure 2: Protein abundance plots of (A) non-enriched and (B) clusterin-enriched human plasma following Protocol 1 for clusterin purification. Proteins were ranked by abundance on the x-axis, while the y-axis displays the average $\log_{10}$-transformed MaxLFQ intensity for each

protein. Each dot represents an individual protein. Selected highly abundant proteins (ALBU, IGHG1, APOA1, and FIBB) were highlighted with CLUS shown in blue.

Workflow optimisation

To improve clusterin purification, all steps of the immunoaffinity purification workflow, including sample loading, washing, and elution conditions, were systematically optimised. To ensure reproducibility and maximise interactions between clusterin and the immobilised antibodies, the affinity resin was kept fully suspended and thoroughly mixed with the sample and buffers at each step of the workflow. In accordance with the supplier's recommendations and to approximate physiological pH, all buffers used for the capture and washing steps were adjusted to pH 7.4, while the elution buffer was maintained at pH 2.3. The pH of the sample was similarly adjusted to approximately 7.4 by diluting 1:1 with DPBS buffer before sample loading. In addition, different incubation times following sample loading onto the affinity resin were tested to evaluate whether prolonged clusterin-resin contact enhanced clusterin enrichment. However, no significant effect was observed across the different tested incubation times (see Figure S1).

Following these adjustments, various washing buffer compositions were evaluated to further optimise clusterin purification by minimising non-specific ionic and hydrophobic protein-protein interactions that contributed to extensive co-purification of plasma proteins. To achieve that, the concentrations of NaCl and Tween 20 in the DPBS washing buffer were systematically varied. NaCl was first evaluated for its ability to suppress ionic interactions by shielding protein surface charges. NaCl was selected because it is a component of DPBS and because both Na^+ and Cl^- ions lie in the centre of the Hofmeister Series, and are therefore expected to exert a minor effect on protein structure and stability[42,43]. Subsequently, Tween 20 was assessed as an additional washing buffer additive to disrupt hydrophobic interactions by coating exposed

hydrophobic regions of proteins, thereby preventing aggregation and non-specific protein-protein interactions involving clusterin[44]. Tween 20 is a non-ionic detergent reported to exert a "renaturating effect" on proteins, referring to its capacity to maintain proteins in solution without inducing denaturation[45]. When evaluated individually, Tween 20 resulted in a greater improvement in clusterin purification than NaCl alone. However, the combined use of both yielded the highest degree of purification (Figure S2).

Multiple combinations of NaCl and Tween 20 concentrations were tested by varying one component at a time while keeping the other constant, to identify conditions that maximised clusterin enrichment. Figure 3 shows the effect of different concentrations of NaCl and Tween 20 on clusterin purification. The detailed purification workflows used are provided in the supporting information (Table S1). As shown in Figure 3A, the relative abundance of clusterin increased with increasing NaCl concentration, reaching a maximum at 0.75 M NaCl. Further increases to 1.0 M and 1.5 M NaCl did not improve purification efficiency but instead led to a decline in clusterin relative abundance. This result likely reflects a salting-in effect, in which a moderate increase in ionic strength shields protein surface charges, reducing protein-protein ionic interactions. However, at higher salt concentrations, competition between salt ions and proteins for water molecules can reduce protein solubility by limiting hydration shell formation around proteins, thereby promoting protein–protein interactions and precipitation[46]. Therefore, higher NaCl concentrations were not tested to avoid potential protein precipitation effects and to prevent interference with mass spectrometry analysis.

In the case of Tween 20 (Figure 3B), progressively increasing its concentration while keeping the NaCl concentration constant enhanced clusterin purification, likely due to the disruption of hydrophobic protein-protein interactions at higher detergent levels[47]. The most substantial improvements were observed with Tween 20 at 0.5%-2%. Specifically, increasing the concentration of Tween 20 from 0.5% to 1% resulted in a 1.6-fold increase in clusterin

relative abundance, followed by an additional 1.1-fold increase when the concentration was further increased to 2%. Raising the Tween 20 concentration to 5% yielded only a minor additional improvement in clusterin purification, despite a 2.5-fold increase in Tween 20 concentration. Considering the limited gain and the aim to avoid protein denaturation[48], 2% Tween 20 was selected as the optimal concentration.

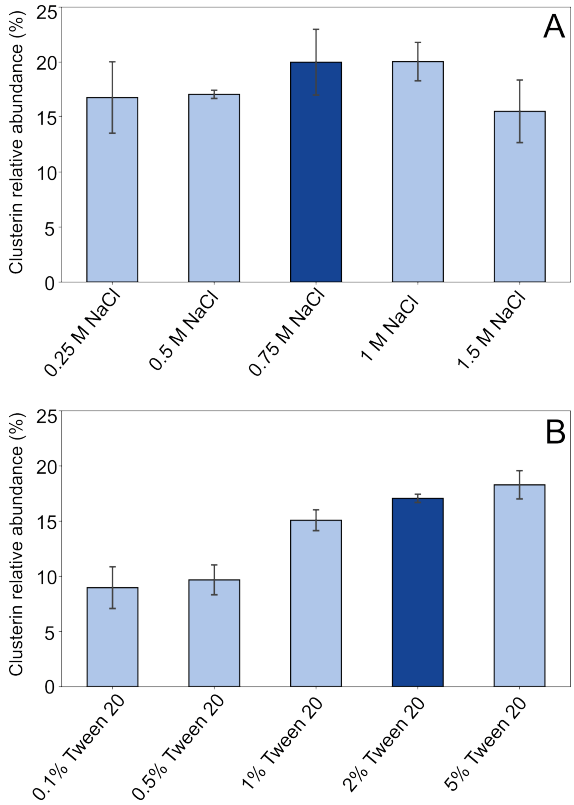

Figure 3: Optimisation of washing buffer composition for clusterin purification. Bar plots show the effect of varying concentrations of (A) Tween 20 and (B) NaCl in the washing buffer on the relative abundance of clusterin. The x-axis indicates the concentrations of NaCl and Tween 20 tested. The y-axis represents the ratio of the $\log_{10}$-transformed MaxLFQ intensity of clusterin to the $\log_{10}$-transformed MaxLFQ intensity of all proteins in the sample, reflecting relative clusterin abundance. During Tween 20 optimisation, the NaCl concentration was held constant at 0.5 M, while during NaCl optimization, the Tween 20 concentration was maintained at 2%. Error bars represent standard deviation across three replicates.

Based on the results, the purification protocol was refined as Protocol 2, which incorporated a total of eight wash steps. After the sample was loaded onto the affinity resin, the first two washes were performed with DPBS containing 0.75 M NaCl and 2% Tween 20, followed by two washes with DPBS containing only 0.75 M NaCl to further reduce protein co-purification and remove residual Tween 20. Subsequently, four consecutive washes with Milli-Q water were implemented to further eliminate remaining Tween 20 and NaCl, ensuring MS compatibility and facilitating the transition to low-pH elution conditions, as Milli-Q water lacks buffering capacity.

After optimising the washing step, the elution buffer composition was also modified to enhance clusterin purification further. To disrupt the interaction between clusterin and antibody, a glycine buffer at pH 2.3 was used, and 0.5 M NaCl was added to improve elution efficiency. The addition of NaCl to the elution buffer resulted in a significant decrease in the co-purification of plasma proteins, as shown in Figure S2D, potentially due to the salting-out effect under acidic conditions. At low pH, most plasma proteins carry a net positive charge and repel one another[49], thereby maintaining their solubility. The addition of salt shields these surface charges, reducing electrostatic repulsion and promoting protein–protein interactions. This increases the likelihood of aggregation or precipitation, thereby lowering protein solubility[46] which could explain the reduction of co-elution of non-target proteins with clusterin.

All the optimisations described above were incorporated into the final purification workflow, referred to as Protocol 3. Compared with the initial protocol (Protocol 1), clear differences were observed in clusterin enrichment and in the extent of plasma proteins co-purified, as illustrated in Figure 4. Using Protocol 1, clusterin was enriched, but extensive co-purification of other plasma proteins was also evident (Figure 4A). In contrast, implementation of the optimised

workflow (Protocol 3) resulted in a drastic reduction in co-purified proteins, indicating substantially improved purification (Figure 4B). Nevertheless, even under the optimised condition of Protocol 3, a small number of proteins co-purified with clusterin, including serum paraoxonase/arylesterase 1 (PON1), cysteine-rich secretory protein 3 (CRIS3), several immunoglobulin variable regions (HV118, HV461, KV315, KVD20), peroxiredoxin-5, mitochondrial (PRDX5), complement C1r subcomponent-like protein (C1RL), and serum amyloid A-1 protein (SAA1). However, their enrichment was substantially lower than that of clusterin, as reflected by smaller fold changes and reduced statistical significance, indicating a weaker and less specific association with the affinity resin.

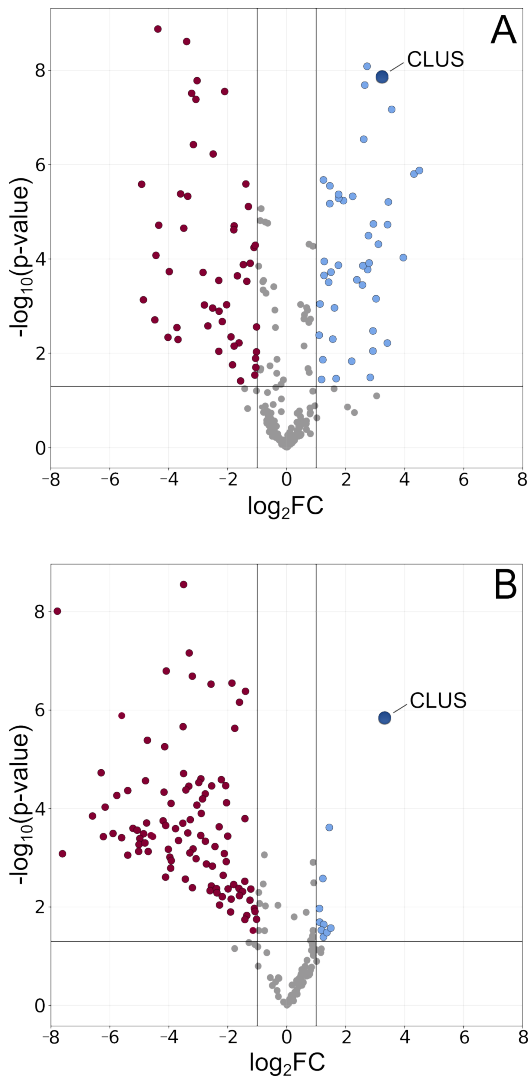

Figure 4: Comparison of clusterin enrichment from human plasma using (A) Protocol 1 and (B) Protocol 3. Volcano plots show $\log_2$ FC (x-axis) versus $-\log_{10}$ (p-value) (y-axis). Proteins significantly enriched by clusterin affinity purification are shown in blue, while proteins detected at higher abundance in non-enriched human plasma are shown in red.

Clusterin Interactome

In addition to purification, the affinity resin was used to study the interactome of clusterin. Under non-disruptive conditions, AP-MS enabled the co-enrichment of clusterin together with its associated proteins, providing insights into clusterin's interaction network in plasma. For interactome analysis, Protocol 1 was used, as it employed mild purification conditions that preserve protein-protein interactions. Following enrichment, clusterin-associated proteins were identified using bottom-up proteomics and subjected to STRING analysis, which facilitated the visualisation of the predicted and experimentally validated interactions between clusterin and other plasma proteins, based on both physical and functional associations[50].

According to the STRING network presented in Figure 5, clusterin was part of an extensive protein-protein interaction network. Clusterin was directly and indirectly associated with numerous proteins, which could be grouped into three categories based on their biological roles, including proteins associated with the hemostasis pathway (red), immune modulation (blue), and high-density lipoprotein particles (HDL; grey).

In detail, the interactome of clusterin comprised numerous proteins associated with HDL particles, complexes composed mainly of phospholipids, cholesterol, and apolipoproteins, whose primary function is to transport lipids, such as cholesterol, between cells[51]. One of the apolipoproteins present in HDL is clusterin (also known as apolipoprotein J), which mainly facilitates the folding of unfolded proteins[52]. Other apolipoproteins associated with HDL that

were present in the network include APOA1, APOB, APOE, APOC4, TTHY, SAA4, PON, GPX3, HPTR, CETP, and PLTP[24,52–59].

In addition to HDL particles, several proteins involved in the hemostasis pathway were also identified within the clusterin interactome. These included proteins such as COMP, THBS, FIBB, FIBA, FINC, VTNC, APOE, FBLN1, THRB, and VWF[60–62]. Additionally, coagulation factors such as F13A, F13B, FA9, and PROC, along with its cofactor PROS1 also participated in the clusterin interactome[60,61,63]. The abundance of hemostasis-related proteins in the interactome of clusterin may be attributed to the role of extracellular chaperones, such as clusterin, in fibrin clots. While not directly participating in the coagulation cascade, chaperones are thought to facilitate the correct folding of unfolded or misfolded proteins, thereby delaying or inhibiting clot formation and exerting a potential anticoagulant effect[64]. Moreover, studies in endothelial cells also suggest a connection between clusterin and the regulation of hemostatic mediators[65,66].

The third group of proteins identified in the interactome included proteins involved in the immune response pathways. This group included proteins such as SAA4 and LBP, which are associated with the innate immune response as acute-phase proteins[67]. Other proteins in this group comprised those participating in the complement cascade, such as CO4A, CO4B, C4BPA, C4BPB, C1S, CO5, and VTNC[68]. The complement system is a vital component in the defence mechanism of the human body, responsible for tagging pathogens for destruction, activating immune cells, and directly eliminating pathogens through the membrane attack complex (MAC) mechanism[69,70]. Vitronectin and clusterin have been reported to inhibit MAC formation, thereby protecting host cells from complement-mediated damage and preventing the lysis of healthy, non-target cells[71], supporting the presence of vitronectin in the clusterin interactome. One exception within the network was SEPP1, which did not fall into any of the three biological groups but was functionally connected to GPX3. Both SEPP1 and GPX3 are

known to be involved in selenium-dependent redox homeostasis[72], explaining SEPP1 presence in the clusterin interactome.

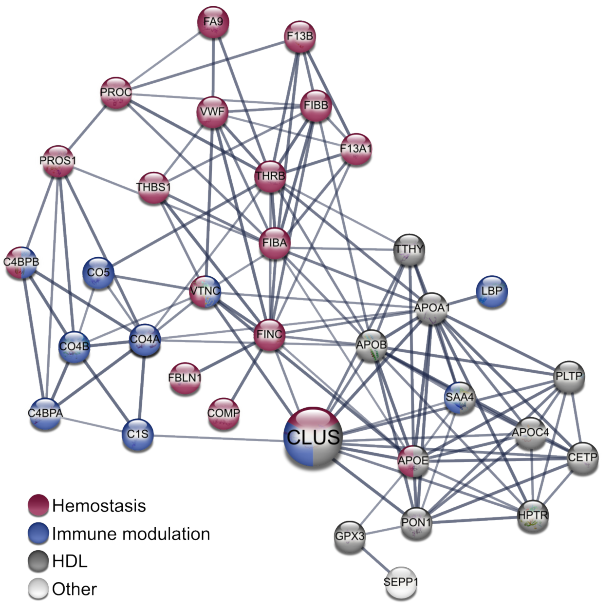

Figure 5: Clusterin interactome in human plasma, visualised using the STRING database. The network comprised 40 proteins significantly enriched following clusterin purification using Protocol 1. The network was mapped based on known and predicted protein–protein interactions. Edges represent confidence scores between proteins, with a minimum required interaction score of 0.700 (high confidence), and edge thickness corresponds to interaction strength. Protein nodes were grouped by biological function: immune modulation (blue), HDL particles (grey), and hemostasis pathway (red). SEPP1 (white) was the only protein in the network not assigned to the aforementioned groups.

Overall, the proposed AP-MS workflow revealed that the interactome of clusterin in human plasma is extensive. Notably, most proteins identified in the analysis have been previously reported as clusterin interaction partners, supporting the specificity of the observed interaction. This suggests that the detected proteins are likely to result from genuine interactions with clusterin or clusterin-containing complexes rather than from nonspecific binding to the affinity

resin, demonstrating that the proposed workflow is suitable for mapping the cluster interactome in complex biological matrices, such as plasma. The complete list of proteins in the network is provided in the Supporting Information (Table S4).

Concluding Remarks

Clusterin is an extracellular chaperone implicated in a wide range of biological processes. Accordingly, analysis of clusterin in human body fluids provides valuable insight into its functional roles in pathological and physiological processes. However, clusterin purification from complex biological matrices remains challenging due to high protein diversity, the presence of highly abundant species, and clusterin's inherent tendency to associate with multiple interaction partners. In this study, we established a versatile workflow combining affinity purification with bottom-up proteomics analysis to enable both targeted purification of clusterin and characterisation of its interactome in human plasma. This approach improves analytical access to clusterin in complex biofluids and enables comprehensive analysis of clusterin-associated proteins in human plasma, providing complementary structural and functional insight into clusterin. Such capabilities are particularly relevant given clusterin's established role in neurodegenerative diseases, such as Alzheimer's and Parkinson's, where it modulates the aggregation of amyloid-β and α-synuclein[16]. Overall, this work establishes the foundation for future studies aiming at linking clusterin-mediated protein interactions to biological functions and disease-related mechanisms.

DATA AVAILABILITY

The LC-MS/MS data and all FragPipe search parameters were deposited to the ProteomeXchange Consortium.

ASSOCIATED CONTENT

Supporting Information.

The supporting information is available free of charge.

Additional experimental details, including detailed purification workflows and buffer compositions (Table S1); parameters of the MS method used (Table S2); protein abundance plot showing the effect of incubation duration post-loading the sample to the affinity resin (Figure S1); protein abundance plots following optimisation of washing and elution buffer compositions (Figure S2); STRING network analysis parameters (Table S3); and a complete list of all proteins identified in the clusterin interactome (Table S4) (PDF).

All combined_protein output files generated by FragPipe for each experimental condition tested (XLXS).

AUTHOR INFORMATION

Corresponding Author

Melissa Baerenfaenger − Division of Bioanalytical Chemistry, Department of Chemistry and Pharmaceutical Sciences, Amsterdam Institute of Molecular and Life Sciences, Vrije Universiteit Amsterdam, 1081 HV Amsterdam, The Netherlands; Centre for Analytical Sciences Amsterdam (CASA), The Netherlands; orcid.org/0000-0002-2855-924X; Email: j.m.baerenfaenger@vu.nl

Authors

Amalia Kontochristou − Division of Bioanalytical Chemistry, Department of Chemistry and Pharmaceutical Sciences, Amsterdam Institute of Molecular and Life Sciences, Vrije Universiteit Amsterdam, 1081 HV Amsterdam, The Netherlands; Centre for Analytical Sciences Amsterdam (CASA), The Netherlands; orcid.org/0009-0006-5988-0024

Nika Šimičić − Division of Bioanalytical Chemistry, Department of Chemistry and Pharmaceutical Sciences, Amsterdam Institute of Molecular and Life Sciences, Vrije Universiteit Amsterdam, 1081 HV Amsterdam, The Netherlands; Centre for Analytical Sciences Amsterdam (CASA), The Netherlands; Center for Proteomics and Metabolomics, Leiden University Medical Center, Leiden 2333, ZA, The Netherlands; orcid.org/0009-0000-4381-6219

Anouk M. Rijs − Division of Bioanalytical Chemistry, Department of Chemistry and Pharmaceutical Sciences, Amsterdam Institute of Molecular and Life Sciences, Vrije Universiteit Amsterdam, 1081 HV Amsterdam, The Netherlands; Centre for Analytical Sciences Amsterdam (CASA), The Netherlands; orcid.org/0000-0002-7446-9907

Author Contributions

The manuscript was written with contributions from all authors. All authors have approved the final version. A. K. contributed to the experimental work, methodology development, conceptualisation, data acquisition, and wrote the original manuscript. N. Š. contributed to methodology development. A. M. R. contributed to supervision, funding acquisition, and manuscript review and editing. M. B. contributed to experimental work, methodology development, supervision, conceptualisation, funding acquisition, and manuscript review and editing.

Notes

The authors declare no competing financial interest.

ACKNOWLEDGMENT

The authors thank Nicolas Laroudie and Dr. Maria Bartel from Thermo Fisher Scientific for their support and input on the development of the clusterin purification workflows. We would also like to thank Dr. Julien Slagboom for his helpful suggestions regarding the affinity purification protocol development, as well as Raya Sadighi and Chuck van der Veen for maintaining the LC and MS instruments used in this study. This research was supported by the Starter Grant provided by the Dutch Ministry of Education, Culture, and Science (OCW).

ABBREVIATIONS

AP-MS, Affinity Purification - Mass Spectrometry; CLUS, Clusterin; DDA-PASEF, Data Dependent - Parallel Accumulation Serial Fragmentation; DPBS, Dulbecco's Phosphate Buffered Saline; ESI, Electrospray Ionisation; FA, Formic acid; FC, Fold Change; HDL, High-density lipoprotein; HPLC, High Performance Liquid Chromatography; LC-MS/MS, Liquid Chromatography Tandem Mass Spectrometry; LFQ-MBR, Label Free Quantification - Match Between Runs; MAC, Membrane Attack Complex; MaxLFQ, Maximum Limit of Quantification; SPE, Solid Phase Extraction; STRING, Search Tool for the Retrieval of Interacting Genes/Proteins; timsTOF, Trapped Ion Mobility Time of Flight.

REFERENCES

1. Satapathy, S.; Wilson, M. R. The Dual Roles of Clusterin in Extracellular and Intracellular Proteostasis. *Trends in Biochem. Sci.* **2021**, *46*, 652–660. DOI: 10.1016/j.tibs.2021.01.005
2. Calero, M.; Tokuda, T.; Rostagno, A.; Kumar, A.; Zlokovic, B.; Frangione, B.; Ghiso, J. Functional and Structural Properties of Lipid-Associated Apolipoprotein J (clusterin). *Biochem. J.* **1999**, *344 (Pt 2)*, 375–383. DOI: 10.1002/1097-0029
3. Yerbury, J. J.; Poon, S.; Meehan, S.; Thompson, B.; Kumita, J. R.; Dobson, C. M.; Wilson, M. R. The extracellular chaperone clusterin influences amyloid formation and

toxicity by interacting with prefibrillar structures. *FASEB J.* **2007**, *21*, 2312–2322. DOI: 10.1096/fj.06-7986com

4. Whiten, D. R.; Cox, D.; Horrocks, M. H.; Taylor, C. G.; De, S.; Flagmeier, P.; Tosatto, L.; Kumita, J. R.; Ecroyd, H.; Dobson, C. M.; Klenerman, D.; Wilson, M. R. Single-molecule characterization of the interactions between extracellular chaperones and toxic α-synuclein oligomers. *Cell Rep.* **2018**, *23*, 3492–3500. DOI: 10.1016/j.celrep.2018.05.074

5. Yuste-Checa, P.; Trinkaus, V. A.; Riera-Tur, I.; Imamoglu, I.; Schaller, T. F.; Wang, H.; Dudanova, I.; Hipp, M. S.; Bracher, A. The extracellular chaperone clusterin enhances Tau aggregate seeding in a cellular model. *Nat. Commun.* **2021**, *12*, 4863. DOI: 10.1038/s41467-021-25060-1

6. Wyatt, A. R.; Yerbury, J. J.; Ecroyd, H.; Wilson, M. R. Extracellular chaperones and proteostasis. *Annu. Rev. Biochem.* **2013**, *82*, 295–322. DOI: 10.1146/annurev-biochem-072711-163904

7. Weinstein, G.; Beiser, A. S.; Preis, S. R.; Courchesne, P.; Chouraki, V.; Levy, D.; Seshadri, S. Plasma clusterin levels and risk of dementia, Alzheimer's disease, and stroke. *Alzheimer's Dement. (Amst.)* **2016**, *3*, 103–109. DOI: 10.1016/j.dadm.2016.06.005

8. Stewart, E. M.; Aquilina, J. A.; Easterbrook-Smith, S. B.; Murphy-Durland, D.; Jacobsen, C.; Moestrup, S.; Wilson, M. R. Effects of glycosylation on the structure and function of the extracellular chaperone clusterin. *Biochemistry* **2007**, *46*, 1412–1422. DOI: 10.1021/bi062082v

9. Trougakos, I. P.; Gonos, E. S. Clusterin/apolipoprotein J in human aging and cancer. *Int. J. Biochem. Cell Biol.* **2002**, *34*, 1430–1448. DOI: 10.1016/s1357-2725(02)00041-9

10. Kovács, P.; Pushparaj, P. N.; Takács, R.; Mobasheri, A.; Matta, C. The clusterin connectome: emerging players in chondrocyte biology and putative exploratory biomarkers of osteoarthritis. *Front. Immunol.* **2023**, *14*, 1103097. DOI: 10.3389/fimmu.2023.1103097

11. Geraghty, N. J.; Satapathy, S.; Wilson, M. R. The emerging roles of extracellular chaperones in complement regulation. *Cells* **2022**, *11*, 3907. DOI: 10.3390/cells11233907

12. Talens, S.; Leebeek, F. W. G.; Veerhuis, R.; Rijken, D. C. Decoration of fibrin with extracellular chaperones. *Thromb. Haemost.* **2019**, *119*, 1624–1631. DOI: 10.1055/s-0039-1693701

13. Fareed, M. M.; Qasmi, M.; Aziz, S.; Völker, E.; Förster, C. Y.; Shityakov, S. The role of clusterin transporter in the pathogenesis of Alzheimer's disease at the blood–brain

barrier interface: a systematic review. *Biomolecules* **2022**, *12*, 1452. DOI: 10.3390/biom12101452

14. Rosenberg, M. E.; Silkensen, J. Clusterin: physiologic and pathophysiologic considerations. *Int. J. Biochem. Cell Biol.* **1995**, *21*, 633–645. DOI: 10.1016/1357-2725(95)00027-m

15. Janiszewska, E.; Kmieciak, A.; Kacperczyk, M.; Witkowska, A.; Kratz, E. M. The influence of clusterin glycosylation variability on selected pathophysiological processes in the human body. *Oxid. Med. Cell. Longev.* **2022**, *2022*, 7657876. DOI: 10.1155/2022/7657876

16. Rodríguez-Rivera, C.; Garcia, M. M.; Molina-Álvarez, M.; González-Martín, C.; Goicoechea, C. Clusterin: always protecting. synthesis, function and potential issues. *Biomed. Pharmacother.* **2021**, *134*, 111174. DOI: 10.1016/j.biopha.2020.111174

17. Tan, J.; Guo, W.; Yang, S.; Han, D.; Li, H. The multiple roles and therapeutic potential of clusterin in non-small-cell lung cancer: a narrative review. *Transl. Lung Cancer Res.* **2021**, *10*, 2683–2697. DOI: 10.21037/tlcr-20-1298

18. Wilson, M. R.; Zoubeidi, A. Clusterin as a therapeutic target. *Expert Opin. Ther. Targets* **2017**, *21*, 201–213. DOI: 10.1080/14728222.2017.1267142

19. Kaur, G.; Poljak, A.; Ali, S. A.; Zhong, L.; Raftery, M. J.; Sachdev, P. Extending the depth of human plasma proteome coverage using simple fractionation techniques. *J. Proteome Res.* **2021**, *20*, 1261–1279. DOI: 10.1021/acs.jproteome.0c00670

20. Poon, S.; Easterbrook-Smith, S. B.; Rybchyn, M. S.; Carver, J. A.; Wilson, M. R. Clusterin is an ATP-independent chaperone with very broad substrate specificity that stabilizes stressed proteins in a folding-competent state. *Biochemistry* **2000**, *39*, 15953–15960. DOI: 10.1021/bi002189x

21. Wilson, M. R.; Roeth, P. J.; Easterbrook-Smith, S. B. Clusterin enhances the formation of insoluble immune complexes. *Biochem. Biophys. Res. Commun.* **1991**, *177*, 985–990. DOI: 10.1016/0006-291x(91)90635-k

22. Bailey, R. W.; Dunker, A. K.; Brown, C. J.; Garner, E. C.; Griswold, M. D. Clusterin, a binding protein with a molten globule-like region. *Biochemistry* **2001**, *40*, 11828–11840. DOI: 10.1021/bi010135x

23. Tousi, F.; Bones, J.; Iliopoulos, O.; Hancock, W. S.; Hincapie, M. Multidimensional liquid chromatography platform for profiling alterations of clusterin N-glycosylation in the plasma of patients with renal cell carcinoma. *J. Chromatogr. A* **2012**, *1256*, 121–128. DOI: 10.1016/j.chroma.2012.07.066

24. Jenne, D. E.; Lowin, B.; Peitsch, M. C.; Böttcher, A.; Schmitz, G.; Tschopp, J. Clusterin (complement lysis inhibitor) forms a high density lipoprotein complex with apolipoprotein A-I in human plasma. *J. Biol. Chem.* **1931**, 266, 11030–11036.

25. Paul, J.; Veenstra, T. D. Separation of serum and plasma proteins for in-depth proteomic analysis. *Separations* **2022**, *9*, 89. DOI:10.3390/separations9040089

26. Millioni, R.; Tolin, S.; Puricelli, L.; Sbrignadello, S.; Fadini, G. P.; Tessari, R.; Arrigoni, G. High abundance proteins depletion vs low abundance proteins enrichment: comparison of methods to reduce the plasma proteome complexity. *PLoS One* **2011**, *6*, e19603. DOI: 10.1371/journal.pone.0019603

27. Wilson, M. R.; Easterbrook-Smith, S. B. Clusterin binds by a multivalent mechanism to the Fc and Fab regions of IgG. *Biochim. Biophys. Acta* **1992**, *1159*, 319–326. DOI: 10.1016/0167-4838(92)90062-i

28. de Silvas, H. V.; Stuart, W. D.; Park, Y. B.; Mao, S. J.; Gil, C. M.; Wetterau, J. R.; Busch, S. J. Harmony, J. A. K. Purification and characterization of apolipoprotein J. *J Biol. Chem.* **1990**, *265*, 14292–14297.

29. Massri, M.; Toonen, E. J. M.; Sarg, B.; Kremser, L.; Grasse, M.; Fleischer, V.; Torres-Quesada, O.; Hengst, L.; Skjoedt, M. O.; Bayarri-Olmos, R.; Rosbjerg, A.; Garred, P.; Orth-Höller, D.; Prohászka, Z.; Würzner, R. Complement C7 and clusterin form a complex in circulation. *Front. Immunol.* **2024**, *15*, 1330095. DOI: 10.3389/fimmu.2024.1330095

30. Jongbloed, W.; Herrebout, M. A. C.; Blankenstein, M. A.; Veerhuis, R. Quantification of clusterin in paired cerebrospinal fluid and plasma samples. *Ann. Clin. Biochem.* **2014**, *51*, 557–567. DOI: 10.1177/0004563213503456

31. Dabbs, R. A.; Wilson, M. R. Expression and purification of chaperone-active recombinant clusterin. *PLoS One* **2014**, *9*, e86989. DOI: 10.1371/journal.pone.0086989

32. Raynes, J. G.; Mcadam, K. P. W. J. Purification of serum amyloid A and other high density apolipoproteins by hydrophobic interaction chromatography. *Anal. Biochem.* **1988**, *173*, 116–124. DOI: 10.1016/0003-2697(88)90168-6

33. Wyatt, A. R.; Wilson, M. R. Identification of human plasma proteins as major clients for the extracellular chaperone clusterin. *J. Biol. Chem.* **2010**, *285*, 3532–3539. DOI: 10.1074/jbc.M109.079566

34. Gordon, S. M.; Deng, J.; Lu, L. J.; Davidson, W. S. Proteomic characterization of human plasma high density lipoprotein fractionated by gel filtration chromatography. *J. Proteome Res.* **2010**, *9*, 5239–5249. DOI: 10.1021/pr100520x

35. Wu, S.; Zhang, S.; Liu, C. M.; Fernie, A. R.; Yan, S. Recent advances in mass spectrometry-based protein interactome studies. *Mol. Cell. Proteomics* **2025**, *24*, 100887. DOI: 10.1016/j.mcpro.2024.100887

36. Cox, J.; Mann, M. Is proteomics the new genomics? *Cell* 2007, *130*, 395–398. DOI: 10.1016/j.cell.2007.07.032

37. Nesvizhskii, A. I. Proteogenomics: concepts, applications and computational strategies. *Nat. Methods* **2014**, *11*, 1114–1125. DOI: 10.1038/nmeth.3144

38. Meier, F; Brunner, A. D.; Koch, S.; Koch, H.; Lubeck, M.; Krause, M.; Goedecke, N.; Decker, J.; Kosinski, T.; Park, M. A.; Bache, N.; Hoerning, O.; Cox, J.; Räther, O.; Mann, M. Online parallel accumulation–serial fragmentation (PASEF) with a novel trapped ion mobility mass spectrometer. *Mol. Cell. Proteomics* **2018**, *17*, 2534–2545. DOI: 10.1074/mcp.TIR118.000900

39. Kong, A. T.; Leprevost, F. V.; Avtonomov, D. M.; Mellacheruvu, D.; Nesvizhskii, A. I.; MSFragger: ultrafast and comprehensive peptide identification in mass spectrometry-based proteomics. *Nat. Methods* **2017**, *14*, 513–520. DOI: 10.1038/nmeth.4256

40. Le Bihan, T.; Nunez de Villavicencio Diaz, T.; Reitzel, C.; Lange, V.; Park, M.; Beadle, E.; Wu, L.; Jovic, M.; Dubois, R. M.; Couzens, A. L.; Duan, J.; Han, X.; Liu, Q.; Ma, B. De novo protein sequencing of antibodies for identification of neutralizing antibodies in human plasma post SARS-CoV-2 vaccination. *Nat. Commun.* **2024**, *15*, 8790. DOI: 10.1038/s41467-024-53105-8

41. Dingess, K. A.; Hoek, M.; van Rijswijk, D. M. H.; Tamara, S.; den Boer, M. A.; Veth, T.; Damen, M. J. A.; Barendregt, A.; Romijn, M.; Juncker, H. G.; van Keulen, B. J.; Vidarsson, G.; van Goudoever, J. B.; Bondt, A.; Heck A. J. R. Identification of common and distinct origins of human serum and breastmilk IgA1 by mass spectrometry-based clonal profiling. *Cell. Mol. Immunol.* **2023**, *20*, 26–37. DOI: 10.1038/s41423-022-00954-2

42. Dumetz, A. C.; Snellinger-O'Brien, A. M.; Kaler, E. W.; Lenhoff, A. M. Patterns of protein–protein interactions in salt solutions and implications for protein crystallization. *Protein Sci.* **2007**, *16*, 1867–1877. DOI: 10.1110/ps.072957907

43. Kang, B.; Tang, H.; Zhao, Z.; Song, S. Hofmeister series: insights of ion specificity from amphiphilic assembly and interface property. *ACS Omega* **2020**, *5*, 6229–6239. DOI: 10.1021/acsomega.0c00237

44. Arsiccio, A.; Pisano, R. Surfactants as stabilizers for biopharmaceuticals: an insight into the molecular mechanisms for inhibition of protein aggregation. *Eur. J. Pharm. Biopharm.* **2018**, *128*, 98–106. DOI: 10.1016/j.ejpb.2018.04.005

45. Zampieri, S.; Ghirardello, A.; Doria, A.; Tonello, M.; Bendo, R.; Rossini, K.; Gambari, P. F. The use of Tween 20 in immunoblotting assays for the detection of autoantibodies in connective tissue diseases. *J. Immunol. Methods* **2000**, *239*, 1–11. DOI: 10.1016/s0022-1759(00)00168-x

46. Nahar, M. K.; Zakaria, Z.; Hashim, U.; Bari, M. F. Effect of pH and salt concentration on protein solubility of slaughtered and non-slaughtered broiler chicken meat. *Sains Malays.* **2017**, *46*, 719–724. DOI:10.17576/jsm-2017-4605-06

47. Chou, D. K.; Krishnamurthy, R.; Randolph, T. W.; Carpenter, J. F.; Manning, M. C. Effects of Tween 20 and Tween 80 on the stability of albutropin during agitation. *J. Pharm. Sci.* **2005**, *94*, 1368–1381. DOI: 10.1002/jps.20365

48. Waters, L. J.; Whiteley, J.; Small, W.; Mellor, S. Determining suitable surfactant concentration ranges to avoid protein unfolding in pharmaceutical formulations using UV analysis. *Heliyon* **2023***, 9*, e21712. DOI: 10.1016/j.heliyon.2023.e21712

49. Pirmoradian, M.; Aarsland, D.; Zubarev, R. Isoelectric point region pI≈7.4 as a treasure island of abnormal proteoforms in blood. *Discoveries (Craiova)* **2016**, *4*, e67. DOI: 10.15190/d.2016.14

50. Szklarczyk, D.; Kirsch, R.; Koutrouli, M.; Nastou, K.; Mehryary, F.; Hachilif, R.; Gable, A. L.; Fang, T.; Doncheva, N. T.; Pyysalo, S.; Bork, P.; Jensen, L. J.; von Mering, C. The STRING database in 2023: protein–protein association networks and functional enrichment analyses for any sequenced genome of interest. *Nucleic Acids Res.* **2023**, *51*, D638–D646. DOI: 10.1093/nar/gkac1000

51. von Eckardstein, A.; Nordestgaard, B. G.; Remaley, A. T.; Catapano, A. L. High-density lipoprotein revisited: biological functions and clinical relevance. *Eur. Heart J.* **2023**, *44*, 1394–1407. DOI: 10.1093/eurheartj/ehac605

52. Brites, F.; Martin, M.; Guillas, I.; Kontush, A. Antioxidative activity of high-density lipoprotein (HDL): mechanistic insights into potential clinical benefit. *BBA Clin.* **2017**, *8*, 66–77. DOI: 10.1016/j.bbacli.2017.07.002

53. Nielsen, M. J.; Petersen, S. V.; Jacobsen, C.; Oxvig, C.; Rees, D.; Møller, H. J.; Moestrup, S. K. Haptoglobin-related protein is a high-affinity hemoglobin-binding plasma protein. *Blood* **2006**, *108*, 2846–2849. DOI: 10.1182/blood-2006-05-022327

54. Zheng, L., Ed. *HDL Metabolism and Diseases*; Springer: Singapore, 2022.

55. Aviram, M.; Rosenblat, M.; Bisgaier, CL.; Newton, R. S.; Primo-Parmo, S. L.; La Du, B. N. Paraoxonase inhibits high-density lipoprotein oxidation and preserves its functions: a possible peroxidative role for paraoxonase. *J. Clin. Invest.* **1998**, *101*, 1581–1590. DOI: 10.1172/JCI1649

56. de Beer, M. C.; Yuan, T.; Kindy, M. S.; Asztalos, B. F.; Roheim, P. S.; de Beer, F. C.Characterization of constitutive human serum amyloid A protein (SAA4) as an apolipoprotein. *J. Lipid Res.* **1995**, *36*, 526–534.

57. Sousa, M. M.; Berglund, L.; Saraiva, M. J. Transthyretin in high density lipoproteins: association with apolipoprotein A-I. *J. Lipid Res.* **2000**, *41*, 58–65. DOI: 10.1016/S0022-2275(20)31271-9

58. Dominiczak, M. H.; Caslake, M. J. Apolipoproteins: metabolic role and clinical biochemistry applications. *Ann Clin Biochem.* **2011**, *48*, 498–515. DOI: 10.1258/acb.2011.011111

59. Zhang, M.; Zhai, X.; Li, J.; Albers, J. J.; Vuletic S, Ren G. Structural basis of the lipid transfer mechanism of phospholipid transfer protein (PLTP). *Biochim. Biophys. Acta Mol. Cell Biol. Lipids.* **2018**, *1863*, 1082–1094. DOI: 10.1016/j.bbalip.2018.06.001

60. Gale, A. J. Current Understanding of Hemostasis. *Toxicol. Pathol.* **2011**, 39, 273–280. DOI: 10.1177/0192623310389474

61. Talens, S.; Leebeek, F. W. G.; Demmers, J. A. A.; Rijken, D. C. Identification of fibrin clot-bound plasma proteins. *PLoS One* **2012**, *7*, e41966. DOI: 10.1371/journal.pone.0041966

62. Liang, Y.; Fu, Y.; Qi, R.; Wang, M.; Yang, N.; He, L.; Yu, F.; Zhang, J.; Yun, C. H.; Wang, X.; Liu, J.; Kong, W. Cartilage oligomeric matrix protein is a natural inhibitor of thrombin. *Blood* **2015**, *126*, 905–914. DOI: 10.1182/blood-2015-01-621292

63. Shah, A. S.; Tan, L.; Long, J. L.; Davidson, W. S. Proteomic diversity of high density lipoproteins: our emerging understanding of its importance in lipid transport and beyond. *J. Lipid Res.* **2013**, *54*, 2575–2585. DOI: 10.1194/jlr.R035725

64. Talens, S.; Leebeek, F. W. G.; Veerhuis, R.; Rijken, D. C. Decoration of Fibrin with Extracellular Chaperones. *Thromb. Haemost.* **2019**, *19*, 1624–1631. DOI: 10.1055/s-0039-1693701

65. van Breevoort, D.; van Agtmaal, E. L.; Dragt, B. S.; Gebbinck, J. K.; Dienava-Verdoold, I.; Kragt, A.; Bierings, R.; Horrevoets, A. J.; Valentijn, K. M.; Eikenboom, J. C.; Fernandez-Borja, M.; Meijer, A. B.; Voorberg. J. Proteomic screen identifies IGFBP7 as a novel component of endothelial cell-specific weibel-palade bodies. *J. Proteome Res.* **2012**, *11*, 2925–2936. DOI: 10.1021/pr300010r

66. Cox, A. A.; Liu, A.; Ng, C. J. Clusterin knockdown has effects on intracellular and secreted von Willebrand factor in human umbilical vein endothelial cells. *PLoS One* **2024**, *19*, e0298133. DOI: 10.1371/journal.pone.0298133

67. Gulhar, R.; Ashraf, M. A.; Jialal, I. Physiology, Acute Phase Reactants. In *Statpearls;* StatPearls Publishing: Treasure Island (FL), 2023.

68. Dunkelberger, J. R.; Song, W. C. Complement and its role in innate and adaptive immune responses. *Cell Res.* **2010**, *20*, 34–50. DOI: 10.1038/cr.2009.139

69. Janeway, C. A., Jr.; Travers, P.; Walport, M.; Shlomchik, M. J. *Immunobiology: the immune system in health and disease*, 5th ed.; Garland Science: New York, 2001.

70. Varela, J. C.; Tomlinson, S. Complement: an overview for the clinician. *Hematol. Oncol. Clin. North Am.* **2015**, *29*, 409–427. DOI: 10.1016/j.hoc.2015.02.001

71. Hallström, T.; Uhde, M.; Singh, B.; Skerka, C.; Riesbeck, K.; Zipfel, P. F. Pseudomonas aeruginosa uses dihydrolipoamide dehydrogenase (Lpd) to bind to the human terminal pathway regulators vitronectin and clusterin to inhibit terminal

pathway complement attack. *PLoS One* **2015**, *10*, e0137630. DOI: 10.1371/journal.pone.0137630

72. Zoidis, E.; Seremelis, I.; Kontopoulos, N.; Danezis, G. P. Selenium-dependent antioxidant enzymes: actions and properties of selenoproteins. *Antioxidants* **2018**, *7*, 66. DOI: 10.3390/antiox7050066